ANALYSIS ON PS-INSAR IN TAIWAN

Jia-Shiang Yang[1] and Jaan-Rong Tsay[*2]
[1]Graduate Student, Department of Geomatics, National Cheng Kung University
1 University Road, Tainan 70101, Taiwan; Tel: +886-6-2370876 # 834
E-mail: moon.shade@msa.hinet.net

[2]Associate Professor Dr.-Ing., Department of Geomatics, National Cheng Kung University
1 University Road, Tainan 70101, Taiwan; Tel: +886-6-2370876 # 838
E-mail: tsayjr@mail.ncku.edu.tw

KEY WORDS: SAR, PS-InSAR, ERS, Subsidence, Displacement Velocity (DV)

ABSTRACT: This paper presents an improved PS-InSAR approach refined from the original one proposed by (Mora et al., 2003), and will analyze the quality and availability of PS-InSAR for determining the subsidence in Taiwan. Some tests are done by using ERS images and some ground truth data in both challenging areas in mid-Taiwan and proper areas in southern Taiwan. In the first areas, the SAR images are acquired before and after the Chi-Chi earthquake. The areas are also covered mostly with dense vegetation. The second areas are located in south Taiwan with continuous subsidence of low velocity and covered with cities and towns. The ground truth data are determined by precise leveling, and are used to evaluate the PS-InSAR results. The precision of the subsidence velocity vectors determined by PS-InSAR in both areas reaches the level of cm/year and mm/year, respectively.

1. INTRODUCTION

Cloud, rain, fog, mist, and haze often emerge in the subtropical area Taiwan throughout the year. About 67% of the island Taiwan is an area of hilly mountains covered with dense vegetation. Disaster events such as earthquakes, debris flows, floods, and landslides often cause sudden high-velocity ground displacements. Moreover, low-velocity subsidence also happens in some local areas in Taiwan. Furthermore, there are over 40 fault lines in Taiwan. These afore-mentioned factors will deteriorate the quality of synthetic aperture radar (SAR) images and decrease the correlation between a pair of SAR images so that they are very challenging and critical to radargrammetry techniques such as persistent scatterer interferometric SAR (PS-InSAR).

Under the before mentioned circumstances, a long-term precise monitoring on the subsidence in Taiwan is very important and necessary. PS-InSAR owns some advantages such as (1) day and night operation for acquiring terrain information, and (2) the ability of penetrating clouds, fogs, rains, and smokes. Nevertheless, some factors such as decorrelation and speckle noises in SAR images will surely decrease the quality of SAR results. Therefore, the applicability of PS-InSAR in Taiwan becomes a headlining research issue.

PS is an existing target which has more stable scattering property and is capable of providing higher coherence in the corresponding SAR image pairs. The phase information from PS is more reliable and can be used in precise interferometry. PS-InSAR extracts as more number of PSs as possible and then estimates the precise displacement velocities (DVs) on these PSs. Dehls et al. (2002) studied the quality of the DV determined by PS-InSAR in Rana, Norway. The result shows that the DVs determined by PS-InSAR can achieve the accuracy level of mm/year. PS-InSAR can evaluate more precisely subsidence velocity vector field in a large area of interest. It owns superior advantages such as that radar wave is able to penetrate cloud, fog, rain and smoke to acquire ground information day and night. However, PS-InSAR suffers seriously the decorrelation problem especially in Taiwan. This decorrelation existing in SAR images is caused by dense coverage of vegetation, longer temporal baseline or large ground displacement and worsens the accuracy of subsidence velocity determined by PS-InSAR.

Ferretti et al. (2000) proposed first a complete PS-InSAR approach to determine the DVs on PSs. Then, the related PS-InSAR approaches have been improved successively e.g. by (Mora et al., 2003), (Hooper et al., 2004) and (Zhang et al., 2011). More recently, PS-InSAR has also been applied and developed in Taiwan. Chou (2008) adopted PS-InSAR to determine the terrain surface DVs in Taipei basin, and concluded that Taipei basin had descended up to 2mm/year from 2003 to 2007. Tung (2008) used PS-InSAR to estimate the subsidence in Yunlin regions, and informed that the subsidence had occurred in this area and the maximum descending DV is about 6cm/year. Siao (2010) adopted adaptable slant range values, instead of a fixed constant slant range in PS-InSAR processing for a computation area,. This method can evaluate more reasonable DVs especially in an area of interest near the boundary of SAR image coverage.

PSs are extracted from PS candidates (PSCs) in PS-InSAR processing. A main advantage of the PS-InSAR method invented by (Mora et al., 2003) is that lots of PSCs can be selected more simply and efficiently by combining coherence images and a specific coherence threshold. Actually, some unfavorable conditions such as land cover of dense vegetation or sudden terrain displacements will surely decrease the coherences of SAR image pairs and increase the difficulty in selecting PSCs. This paper presents an improved PS-InSAR approach refined from the original one proposed by (Mora et al., 2003). Test results demonstrate that it is capable of obtaining more applicable PSCs. Section 2 will tersely state the improved PS-InSAR approach. Section 3 illustrates the PS-InSAR test in central Taiwan with unfavorable conditions. The improved PS-InSAR is validated by comparing the results with ground truth data determined by precise leveling. A control group versus the experiment group shown in section 3 is demonstrated in section 4. The test area located in Tainan city has crowded buildings, stable and continuous displacements and no sudden high-velocity displacement during the acquisition time duration of SAR images. The valuable applicability of the improved PS-InSAR approach is highlighted by comparing the results summarized in the sections 3 and 4.

2. AN IMPROVED PS-INSAR APPROACH

First, some SAR images in an area of interest must be acquired. A master SAR image must then be selected, and the others are registered with the master image to generate the corresponding coherence images and interferograms. Actually, both topography and displacement effects are contained in the interferograms. The topography effects are removed from the interferograms by using differential interfering to generate the differential interferograms. Then, PS-InSAR utilizes the differential interferometric phases on PSs to estimate the corresponding DVs. The PSs with higher coherence values can provide more reliable phase information to PS-InSAR.

When two SAR images are registered successfully, the two conjugate pixel values can be expressed respectively as

$$P_1 = x_1 + j \cdot y_1 \tag{1}$$

$$P_2 = x_2 + j \cdot y_2 \tag{2}$$

where x_1, x_2, y_1 and y_2 are all real numbers, and $j=\sqrt{-1}$. The coherence value can then be expressed as (Rosen et al., 2000)

$$C = \frac{\left| E\left[P_1 \cdot P_2^*\right] \right|}{\sqrt{E\left[P_1 \cdot P_1^*\right] \cdot E\left[P_2 \cdot P_2^*\right]}} \tag{3}$$

where P_1^* and P_2^* are the complex conjugates of P_1 and P_2 and $E[\ ]$ means the expectation value. The defined coherence values range thus from 0 to 1.

The PSCs have to be selected before extracting the PSs. Mora et al. (2003) adopts a coherence threshold to select PSCs. Accordingly, only an object point, whose coherence values on all SAR images are larger than the threshold, is selected as a PSC. The improved method for selection of PSCs is refined from the general one mentioned above. Perpendicular baseline is the vertical component of spatial baseline between two SAR images. Independent of interferometric geometry, those PSs on the SAR images with shorter perpendicular baselines have persistently higher coherences (Ferretti et al., 2000; Mora et al., 2003). Therefore, only the coherence images with shorter perpendicular baselines are used to select PSCs in our improved approach. Then the criterion of perpendicular baseline length isn't taken into account any more, and all differential interferograms are involved in extracting the PSs and estimating the DVs. This improved PS-InSAR approach is helpful especially to the PS-InSAR case with unfavorable conditions.

The method of Delaunay triangulation is employed to connect the PSCs and thus to build the phase structure. The differential interferometric phases which come from the several adopted differential interferograms build the phase structure. A linear model is utilized to fit this phase structure. Then, an adjustment is used to solve this linear model for first extracting the PSs and then evaluating the linear DVs on these PSs. In fact, these linear DVs are relative to each other. The so-called model coherence values (Ferretti et al., 2000) on the connected PSCs can be obtained after the adjustment is done and range from 0 to 1. Model coherence value is equal to 1 when the adjustment result is most precise. Oppositely, model coherence value equals 0 in the case of total decorrelation so that the adjustment failed entirely. The PSCs with the model coherence values larger than or equal to 0.7 (Mora et al., 2003) is extracted as the PSs.

Then, a region growing algorithm proposed by (Xu and Cumming, 1999) is used to retrieve the linear DV on each PS. This technique starts operating from several seed pixels with higher model coherence values. Then this region growing algorithm estimates the linear DV on a specific PS by

$$v_{estimated}(x,y)=\frac{1}{\sum_p r_{Model}(x,y,x_p,y_p)}\cdot\sum_p\left(\left(v_{estimated}(x_p,y_p)+\Delta v_{estimated}(x,y,x_p,y_p)\right)\cdot r_{Model}(x,y,x_p,y_p)\right) \quad (4)$$

(x,y) are the local two-dimensional plane coordinates of this PS. p denotes the neighboring PSs which are connected to this PS. $\Delta v_{estimated}$ means the increment of DV. r_{Model} is the model coherence value which is regarded as the weighting value to reduce the contributions of those less reliable connections on evaluating $v_{estimated}(x,y)$.

3. EVALUATING THE SUBSIDENCE IN CENTRAL TAIWAN

3.1 Test Data

Figure 1 illustrates the test area in central Taiwan inclusive of Miaoli, Taichung, Changhua, Yunlin and Nantou regions. The subsidence database available on the website http://www.subsidence.org.tw/index2.aspx shows that Changhua and Yunlin are subsiding areas in 1999. This area of 72km x 72km is covered mostly with vegetation. In this case, the coherences of the SAR image pairs are reduced so that the difficulty in selecting sufficient number of applicable PSCs is encountered unavoidably.

Figure 1 Test area (this figure is revised from http://fault.moeacgs.gov.tw/MGFault/ Default.aspx)

Table 1 lists some attributes of the SAR image pairs adopted in this test. Temporal baseline means the time difference between two SAR image acquisitions. The SAR images of 600×600 pixels are acquired on the European Remote-Sensing satellite 2 (ERS-2) and have the ground resolution of 120m. The master SAR image, acquired on May 6, 1999, is denoted by the blue characters. The other slave SAR images are registered then with the master one to form the eight SAR image pairs. Actually, the Chi-Chi earthquake occurred on September 21, 1999 between the acquisition dates of the two SAR images 1999/08/19 and 1999/09/23 denoted by the red characters. Test result demonstrates that the improved PS-InSAR approach can still produce the DVs with a specific accuracy level even if the earthquake deteriorates the quality of interferograms and reduces the coherence values of SAR image pairs.

Table 1 Some attributes of the SAR image pairs

SAR Image Source	Acquisition Date	Perpendicular Baseline (m)	Temporal Baseline (days)
ERS-2 Satellite	1999/01/21	91.2	-105
ERS-2 Satellite	1999/04/01	318.9	-35
ERS-2 Satellite	1999/05/06	/	/
ERS-2 Satellite	1999/06/10	116.4	35
ERS-2 Satellite	1999/07/15	248.4	70
ERS-2 Satellite	1999/08/19	319.4	105
ERS-2 Satellite	1999/09/23	54.2	140
ERS-2 Satellite	1999/10/28	36.0	175
ERS-2 Satellite	1999/12/02	490.6	210

3.2 Selecting PSCs and Computing Vertical DVs

The coherence threshold 0.25 suits for most PS-InSAR cases (Mora et al., 2003), and it is also utilized here to select the PSCs. In this case, no PSC is selected in our test area. Nevertheless, the improved PS-InSAR approach adopts only those four coherence images with the perpendicular baseline shorter than 200m. The perpendicular baseline less than 200m is more suitable for interferometry case (Ferretti et al., 2000) because the corresponding interferogram has higher coherences independent of interferometric geometry. The four SAR image pairs

coincident with the aforementioned criterion are picked out. Finally, there are altogether 9422 PSCs to be selected successfully and illustrated by the white dots in figure 2.

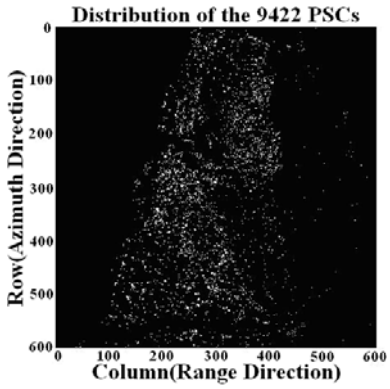

Figure 2 Locations of the 9422 PSCs

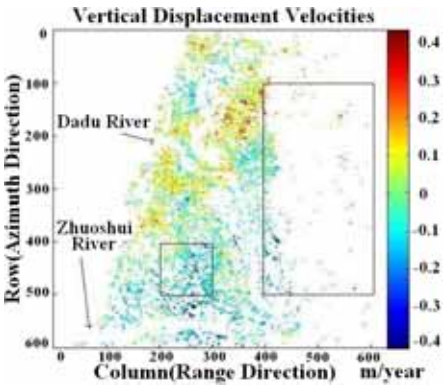

Figure 3 Vertical DVs

Then, the eight differential interferograms are computed from the original interferograms by using differential interfering. The topography pair is composed of the two SAR images of tandem mode acquired on March 6, 1996 and March 7, 1996. These two SAR images have the temporal baseline of only one day so that they provide the interferometric phases with higher coherences and more reliable phase component of topography effect.

After the eight differential interferograms are applied to the PS-InSAR processing, the 9196 PSs are extracted from the 9422 PSCs and their vertical DVs are illustrated in figure 3. The plus and minus values indicate respectively the ascending and descending DVs with the unit m/year in 1999. The left and right rectangles in figure 3 denote a plain and mountainous area, respectively. The PS densities in the plain and mountain areas are 5.72PS/km^2 (823PS/144km^2) and 0.44PS/km^2 (502PS/1152km^2), respectively. Both subsidence and Chi-Chi earthquake cause the ground displacement events in this test area. Evidently, PS-InSAR results show that most PSs located in Changhua and Yunlin regions are descending. This finding agrees with the conclusion drawn from the precise leveling, namely that the subsidence occurred in Changhua and Yunlin regions in 1999.

The vertical DVs determined by precise leveling on benchmarks are available from the subsidence database and are used as the ground truth data. Table 2 shows the average vertical DVs, estimated respectively from ground truth data and PS-InSAR results, in 1999 in Lukang, Fangyuan and Tacheng areas. The PS densities are 2.89PS/km^2 (520PS/180km^2), 1.54PS/km^2 (533PS/345.6km^2) and 0.84PS/km^2 (145PS/172.8km^2) in Lukang, Fangyuan and Tacheng areas, respectively. Both results are consistent, namely ascending in Lukang area and descending in Fangyuan and Tacheng areas. Therefore, the improved PS-InSAR approach is validated.

Table 2 The average vertical DVs in 1999 in Lukang, Fangyuan and Tacheng areas

Area	Lukang	Fangyuan	Tacheng
Ground Truth Data	+2.3cm/year	-3.3cm/year	-7.3cm/year
PS-InSAR Result	+5.3cm/year	-5.5cm/year	-4.7cm/year

3.3 Computation Precision

Table 3 The computation precision estimated by RMSD in six local small areas in central Taiwan

	Area1	Area2	Area3	Area4	Area5	Area6
area (km^2)	5.76	0.50	0.23	2.16	1.44	0.52
PS Density (PS/km^2)	3.65	28.00	56.52	6.48	11.11	17.31
Displacement Tendency	Ascending	Ascending	Ascending	Descending	Descending	Descending
RMSD (cm/year)	4.09	3.08	2.90	3.23	4.99	3.19
Average Coherence Value	0.31	0.34	0.30	0.25	0.24	0.25

The computation precision is estimated by RMSD in six local small areas where vertical DVs are relatively consistent. These smaller areas are located in cities and own relatively higher coherences. Table 3 lists the RMSDs. In general, the denser the PSs in an area, the smaller the RMSD. Actually, the condition of the test area is disadvantageous for PS-InSAR. The unfavorable conditions reduce the coherence and deteriorate the precision of

DVs determined by PS-InSAR. Table 3 shows that the average coherence values are lower and range from 0.24 to 0.34. The areas which are more suitable for estimating RMSD are picked up as more as possible. The average RMSD estimated from these six areas is 3.58cm/year. In other word, PS-InSAR estimates the displacement velocity vectors in the central Taiwan with the precision of about 4cm/year.

4. ESTIMATING THE DISPLACEMENT VELOCITY IN TAINAN CITY

Figure 4 illustrates another test area of 8km x 8km in Tainan city. Comparing to the aforementioned test area in central Taiwan, this test area has more favorable conditions. Most of this area is covered with dense buildings and is capable of providing higher coherence for interferometry.

Figure 4 Test area in Tainan

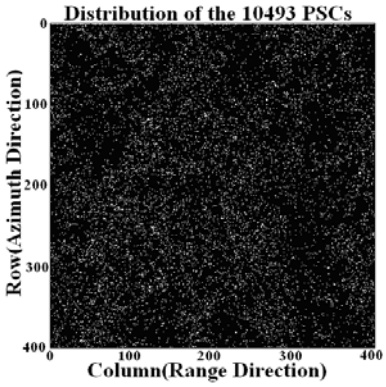

Figure 5 Locations of 10493 PSCs

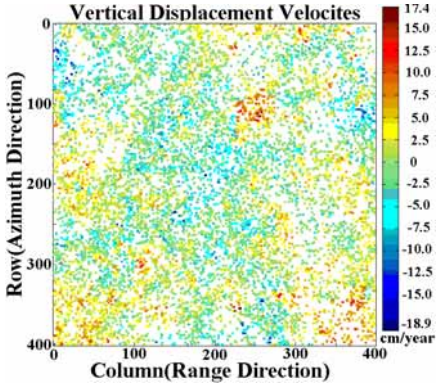

Figure 6 Vertical DVs

(Figure 4 is edited from http://fault.moeacgs.gov.tw/MGFault/ Default.aspx)

Some attributes of the SAR image pairs are shown in table 4. The SAR images cover 400 x 400 pixels and have the 20m ground resolution, and the one acquired on May 6, 1999 is taken as the master image denoted by the blue characters. These SAR images are acquired before the Chi-Chi earthquake so that the coherences of SAR image pairs are not deteriorated by the sudden large ground displacement. Table 4 shows clearly that these SAR images have in general longer perpendicular baselines than the ones in the aforementioned test areas in central Taiwan. In total, 10493 PSCs are selected successfully even merely by using the general method with the coherence threshold 0.40, and their locations are shown in figure 5. Adopting the coherence threshold 0.40 can obtain sufficient number of PSCs with higher coherence values for the follow-up PS-InSAR processing. Finally, the 10204 PSs are selected and their corresponding vertical DVs are computed and illustrated in figure 6. The PS density is 150.06PS/km^2 and much larger than 5.72PS/km^2 for the plain area in central Taiwan shown in the first PS-InSAR test described in section 3.

Table 4 Some attributes of the SAR image pairs used in the test area Tainan

SAR Image Source	Acquisition Date	Perpendicular Baseline (m)	Temporal Baseline (days)
ERS-2 Satellite	1998/11/12	-87.2	-175
ERS-2 Satellite	1998/12/17	-885.8	-140
ERS-2 Satellite	1999/01/21	-95.3	-105
ERS-2 Satellite	1999/04/01	-809.3	-35
ERS-2 Satellite	1999/05/06	/	/
ERS-2 Satellite	1999/06/10	-407.4	35
ERS-2 Satellite	1999/07/15	-253.7	70
ERS-2 Satellite	1999/08/19	776.3	105

Table 5 The computation precision estimated by RMSD in six areas in Tainan city

	Area1	Area2	Area3	Area4	Area5	Area6
PS Density (PS/km^2)	183.33	233.33	175.00	233.33	190.91	150.00
Displacement Tendency	Ascending	Ascending	Ascending	Descending	Descending	Descending
RMSD (cm/year)	1.63	1.62	1.31	1.92	1.78	0.83
Average Coherence Value	0.66	0.69	0.66	0.63	0.69	0.63

Table 5 lists some statistic figures on computation precisions. Comparing table 5 with table 3, it is clear that the PSs are significantly much denser in Tainan City area than the ones in the test areas in central Taiwan described in section 3. The global average coherence values are 0.28 and 0.66 for the test areas central Taiwan and Tainan, respectively. The difference on these two global average coherence values is significant. Also, the average RMSDs in table 3 and 5 are 3.58cm/year and 1.52cm/year, respectively. Moreover, one of the six RMSDs in table 5 is 0.83cm/year which achieves the precision level of mm/year. Briefly to say, the precision of the DVs determined by PS-InSAR in areas with more favorable conditions and higher coherence is much better.

5. CONCLUSIONS AND FUTURE WORKS

An improved PS-InSAR approach is proposed and validated. It adds an advantageous criterion into the general PS-InSAR method to select more applicable PSCs in an interest area with unfavorable conditions. The improved PS-InSAR approach extracts successfully the 9196 PSs from the unfavorable area where no PSC can be obtained by using the general PS-InSAR method. The average RMSDs in the unfavorable area central Taiwan and favorable area Tainan City, both with the average coherence values of 0.28 and 0.66, are respectively 3.58cm/year and 1.52cm/year. Furthermore, in a portion of Tainan City area, PS-InSAR determines DVs with the precision 0.83cm/year which reaches the level of mm/year. Briefly to say, the precision of the DVs determined by PS-InSAR in areas with more favorable conditions and higher coherence is much better. In the near future, some related issues on PS-InSAR and its integration with other techniques will be further developed and studied for the application purpose of high-precision subsidence monitoring in Taiwan.

REFERENCE

Chou, F. M., 2008. Measurement of Surface Deformation in Northern Taiwan by Using PSInSAR Techniques. Master's Thesis, National Central University, Taoyuan, Taiwan.

Dehls, J., Basilio, M. and Colesanti, C., 2002. Ground Deformation Monitoring in the Ranafjord Area of Norway by Means of the Permanent Scatterer Technique. International Geoscience and Remote Sensing Symposium, Toronto, Canada, June 24-28, Vol. 1, pp. 203-207.

Ferretti, A., Prati, C., and Rocca, F., 2000. Nonlinear Subsidence Rate Estimation Using Permanent Scatterers in Differential SAR Interferometry. IEEE Transactions on Geoscience and Remote Sensing, Vol. 38, No. 5, pp. 2202-2212.

Hooper, A., Zebker, H., Segall P. and Kampes, B., 2004. A New Method for Measuring Deformation on Volcanoes and Other Natural Terrains Using InSAR Persistent Scatterers. Geophysical Research Letters, Vol. 31, L23611.

Mora, O., Mallorqui, J. J. and Broquetas, A., 2003. Linear and Nonlinear Terrain Deformation Maps from a Reduced Set of Interferometric SAR Images. IEEE Transactions on Geoscience and Remote Sensing, Vol. 41, No. 10, pp. 2243-2253.

Rosen, P. A., Hensley, S., Joughin, I. R., Li, F. K., Madsen, S. N., Rodriguez, E. and Goldstein, R. M., 2000. Synthetic Aperture Radar Interferometry-Invited Paper. Proceedings of IEEE, Vol. 88, Issue 3, pp.333-382.

Siao, Y. F., 2010. Detection of Surface Displacements by a PSInSAR Technique. Master's Thesis, National Central University, Taoyuan, Taiwan.

Tung, H., 2008. Analysis of Surface Deformation based on PS-InSAR Technique: Case Studies in Coastal Plain, SW Taiwan. Master's Thesis, National Taiwan University, Taipei, Taiwan.

Xu W. and Cumming I., 1999. A Region-Growing Algorithm for InSAR Phase Unwrapping. IEEE Transactions on Geoscience and Remote Sensing, Vol. 37, Issue 1, pp. 124-134.

Zebker, H. A., Rosen, P. A., Goldstien, R. M., Gabriel, A. and Werner, C. L., 1994. On the Derivation of Coseismic Displacement Fields Using Differential Radar Interferometry: The Landers Earthquake. Journal of Geophysical Research, Vol. 99, No. B10, pp. 19617-19634.

Zhang, L., Ding, X. and Lu, Z., 2011. Ground Settlement Monitoring Based on Temporarily Coherent Points between Two SAR Acquisitions. ISPRS Journal of Photogrammetry and Remote Sensing, Vol. 66, Issue 1, pp. 146-152.